Role of Actin DNase-I-Binding Loop in Myosin Subfragment 1-Induced Polymerization of G-actin: Implications for the Mechanism of Polymerization

Barbara Wawro,* Sofia Yu. Khaitlina,† Agnieszka Galińska-Rakoczy,* and Hanna Strzelecka-Gołaszewska*
*Department of Muscle Biochemistry, Nencki Institute of Experimental Biology, Warsaw, Poland; and †Department of Cell Culture, Institute of Cytology, St. Petersburg, Russia

ABSTRACT Proteolytic cleavage of actin between Gly^{42} and Val^{43} within its DNase-I-binding loop (D-loop) abolishes the ability of Ca-G-actin to spontaneously polymerize in the presence of KCl. Here we show that such modified actin is assembled into filaments, albeit at a lower rate than unmodified actin, by myosin subfragment 1 (S1) carrying the A1 essential light chain but not by S1(A2). S1 titration of pyrene-G-actin showed a diminished affinity of cleaved actin for S1, but this could be compensated for by using S1 in excess. The most significant effect of the cleavage, revealed by measuring the fluorescence of pyrene-actin and light-scattering intensities as a function of actin concentration at saturating concentrations of S1, is strong inhibition of association of G-actin-S1 complexes into oligomers. Measurements of the fluorescence of dansyl cadaverine attached to Gln^{41} indicate substantial inhibition of the initial association of G-actin-S1 into longitudinal dimers. The data provide experimental evidence for the critical role of D-loop conformation in both longitudinal and lateral, cross-strand actin-actin contact formation in the nucleation reaction. Electron microscopic analysis of the changes in filament-length distribution during polymerization of actin by S1(A1) and S1(A2) suggests that the mechanism of S1-induced polymerization is not substantially different from the nucleation-elongation scheme of spontaneous actin polymerization.

INTRODUCTION

Numerous functions of the actin cytoskeleton in eukaryotic cells are based on its ability to undergo quick rearrangements in response to extracellular and intracellular signals. These rearrangements result from actin polymerization or depolymerization that is temporarily and spatially regulated by a variety of actin-binding proteins. There is a growing body of evidence that these regulatory proteins accomplish their tasks by making use of the intrinsic structural flexibility of actin (Egelman and Orlova, 1995), and of the known principles of actin polymerization in the presence of ATP (Carlier and Pantaloni, 1997).

Atomic models of F-actin filament (Holmes et al., 1990; Lorenz et al., 1993; Tirion et al., 1995) confirm that the filament structure is stabilized by ''longitudinal'' contacts between subunits of the same strand, and by ''lateral'' contacts between subunits of the two strands of the long-pitch F-actin helix, as predicted by the model of helical polymerization (Oosawa and Kasai, 1962). Salt-induced polymerization of actin follows a monomer activation-nucleation-filament growth scheme, with nucleation being the rate-limiting step (for a review, see Carlier, 1991). Theoretical considerations and kinetic analyses of polymerization indicate that the smallest oligomer that can grow into a filament is a trimer (e.g., Oosawa and Kasai, 1962; Kasai et al., 1962; Cooper et al., 1983a; Frieden, 1983). According to Brownian dynamics simulations and binding free-energy calculations, the most critical step in the nucleation process is formation of a longitudinal dimer that is, however, still unstable and easily dissociates until it is stabilized by lateral interactions with a third monomer, initiating the second strand of F-actin subunits (Sept and McCammon, 2001).

At low ionic strength, actin can be polymerized by myosin subfragments, heavy meromyosin, or subfragment 1 (S1). Although the S1-induced polymerization has been extensively studied over more than a decade, the details of its mechanism are still controversial. Experimental data from two laboratories indicate a 1:1 binding stoichiometry of the two proteins in both the initial acto-S1 complexes and the final S1-decorated filaments (Miller et al., 1988; Lheureux et al., 1993; Kasprzak, 1993; Kim et al., 1998). From this and other findings, it has been concluded that binary G-actin-S1 (GS) complexes assemble into filaments according to the monomer activation-nucleation-filament growth scheme (Miller et al., 1988; Chen et al., 1992; Lheureux et al., 1993). An entirely different mechanism has been proposed by Carlier and her colleagues. Analysis of acto-S1 complexes formed in the absence of ATP and kinetic considerations have led these authors to suggest that S1 sequentially binds two actin molecules, the resulting ternary G_2S complexes undergo rapid and massive self-condensation into short helical oligomers, and these yield S1-decorated actin filaments by slower end-to-end annealing. Although incorporation of binary GS complexes into oligomers has also been predicted in this model, the main route involves oligomerization of G_2S and further binding of S1 up to the 1:1 molar ratio during oligomer

Submitted July 8, 2004, and accepted for publication December 29, 2004.

Address reprint requests to Hanna Strzelecka-Gołaszewska, Dept. of Muscle Biochemistry, Nencki Institute of Experimental Biology, 3 Pasteur St., 02-093 Warsaw, Poland. Tel.: 48-22-589-2309; Fax: 48-22-822-5342; E-mail: hannas@nencki.gov.pl.

0006-3495/05/04/2883/14 $2.00

doi: 10.1529/biophysj.104.049155

annealing (Valentin-Ranc et al., 1991; Valentin-Ranc and Carlier, 1992; Blanchoin et al., 1995; Fievez et al., 1997a). In view of the interaction of each S1 with two adjacent actin subunits along the same long-pitch helical strand of subunits in S1-decorated F-actin filament (Rayment et al., 1993), it has been assumed that the G_2S complex is characterized by longitudinal actin-actin interactions with respect to the future filament axis, and that actin-actin contacts along the genetic helix (lateral contacts) appear in the oligomers.

Similar to the nucleation of ATP-G-actin in salt-induced polymerization, the rate-limiting step of condensation of the initial acto-S1 complexes into oligomers is stimulated by the presence of Mg^{2+} at the high-affinity site in actin (Fievez et al., 1997b). It has also been shown that the acceleration of S1-induced polymerization by myosin A1 light chain (Chen and Reisler, 1991; Valentin-Ranc et al., 1991; Lheureux et al., 1993) is due to a higher equilibrium constant for oligomerization of the complexes formed with the S1(A1) isoform (Valentin-Ranc and Carlier, 1992). Whereas the effects of bound Ca^{2+}/Mg^{2+} can only be explained in terms of a cation-dependent change in actin conformation, the molecular basis of the effect of myosin A1 light chain is not yet fully understood.

The atomic models of F-actin structure (Holmes et al., 1990; Lorenz et al., 1993; Tirion et al., 1995 predict a direct participation of the DNase-I-binding loop (D-loop, residues 38–52) on the top of subdomain 2 of actin in the intrastrand interactions between F-actin subunits. Modeling of the F-actin structure has also led to the ''hydrophobic pocket-plug'' hypothesis suggesting that these longitudinal interactions create a hydrophobic pocket into which intercalates the hydrophobic loop 262–274 of an adjacent subunit from the opposite strand (Holmes et al., 1990; Lorenz et al., 1993). Formation of an intermolecular interface in F-actin between the N-terminal portion of the D-loop, actin C-terminus, and the 262–274 ''plug'' was confirmed by spectroscopic and chemical cross-linking studies (Kim et al., 2000; Kim and Reisler, 1996 and 2000; Feng et al., 1997). It implies a role of D-loop in stabilization of both longitudinal and lateral intersubunit contacts. We have previously shown that proteolytic cleavage of this loop between Gly^{42} and Val^{43} strongly inhibits salt-induced polymerization of actin (Khaitlina et al., 1991, 1993) and stimulates the turnover of F-actin subunits, indicating a substantial weakening of intersubunit interactions (Khaitlina and Strzelecka-Gołaszewska, 2002). In this work, we made use of this modification of actin to evaluate the contribution of the D-loop to longitudinal and lateral contact formation in the process of actin polymerization. This question seems to be of interest because the motile processes based on actin polymerization are frequently initiated by de novo filament formation. We have focused on polymerization induced by S1 because the reported massive association of initial actin-S1 complexes into oligomers enables quantitation of these intermediates of polymerization (Valentin-Ranc and Carlier, 1992), whereas the small amounts of transiently formed nuclei in salt-induced polymerization are not detectable. In turn, the polymerization properties of modified actin revealed in this work proved useful in getting a new insight into the mechanism and, in particular, the role of myosin A1 light chain in S1-induced polymerization.

MATERIALS AND METHODS

Chemicals

EGTA, HEPES, MOPS, and ATP were from Sigma Chemical (St. Louis, MO). *N*-(1-pyrenyl)iodoacetamide and dansyl cadaverine were purchased from Molecular Probes (Eugene, OR). SP-Trisacryl M was obtained from BioSepra (Sergy-Saint-Christophe, France). All other chemicals were of analytical grade.

Protein preparations

Rabbit skeletal muscle actin, isolated from acetone-dried muscle powder was purified according to Spudich and Watt (1971) and, additionally, by gel filtration on Sephadex G-100 and was stored at 4°C in a buffer containing 2 mM HEPES, pH 7.6, 0.2 mM ATP, 0.1 mM $CaCl_2$, 0.2 mM DTT, and 0.02% NaN_3 (buffer G). Labeling of actin at Cys^{374} with *N*-(1-pyrenyl)iodoacetamide was performed as described by Cooper et al. (1983b). Labeling with dansyl cadaverine (DC) at Gln^{41} via a transglutaminase reaction (Takashi, 1988) was preformed as described by Moraczewska et al. (1999). Unbound fluorophores and protein aggregates were removed by gel filtration on a Sephadex G-100 column using buffer G as an eluant. Actin specifically cleaved between Gly^{42} and Val^{43} (Khaitlina et al., 1991), both unlabeled and fluorescently labeled, was prepared by limited digestion with protease ECP32 from *Escherichia coli* A2 strain (ECP), as described previously (Khaitlina et al., 1993). The proteolytically modified actins were used within 1 day. Chymotryptic S1 was prepared from rabbit skeletal muscle myosin as described by Margossian and Lowey (1982). Isoforms S1(A1) and S1(A2) were separated by ion-exchange chromatography on SP-Trisacryl M (Trayer and Trayer, 1988), concentrated using Centriprep Centrifugal Filter Devices (Amicon, Millipore Co., Bedford, MA), and stored at 2°C in 10 mM MOPS, pH 7.0, 80 mM NaCl, and 0.4 mM DTT for up to 4 days. Before use, the preparations were dialyzed against ATP-free buffer G and clarified by 0.5 h centrifugation at 300,000 × *g*. Typical electrophoretic patterns of the protein preparations used throughout this work (SDS-PAGE according to Laemmli, 1970) are shown in Fig. 1.

Protein concentrations were determined spectrophotometrically using an absorption coefficient of 0.63 ml mg^{-1} cm^{-1} at 290 nm for G-actin (Houk and Ue, 1974) and 0.75 ml mg^{-1} cm^{-1} at 280 nm for S1 (Margossian and Lowey, 1982).

Preparation of phalloidin-stabilized F-actin seeds

Unmodified Ca-G-actin (50 μM) was polymerized with 0.1 M KCl in the presence of equimolar phalloidin. Seeds were produced by fragmentation of the obtained polymers by injection, through a microsyringe needle, of a small volume (5 μl) of the polymer solution into 995 μl of G-actin solution several seconds before addition of salt to start polymerization.

Light-scattering and fluorescence measurements

The measurements were carried out in a Spex Fluorolog spectrofluorometer (Spex Industries, Edison, NJ). Light-scattering measurements were taken at a 90° angle, at 365 nm. Excitation and emission wavelength for pyrene fluorescence measurements were set, respectively, at 365 nm and 407 nm, and those for dansyl fluorescence at 332 nm and 525 nm.

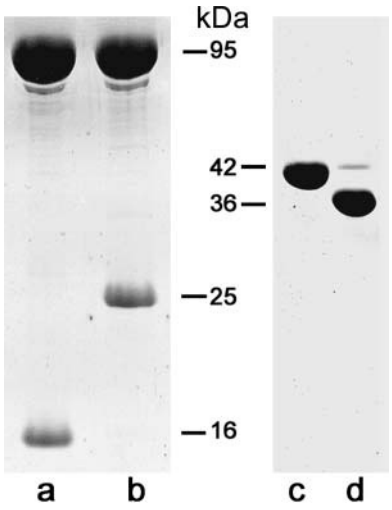

FIGURE 1 Sodium dodecyl sulfate polyacrylamide gel electrophoresis of the protein preparations used throughout this work. (*a* and *b*) S1(A2) and S1(A1), respectively; electrophoresis on a 15% (mass/vol) gel slab. (*c* and *d*) Unmodified and ECP-cleaved actin, respectively; electrophoresis on a 12% gel slab. The fast-migrating N-terminal fragment of ECP-cleaved actin is not visualized under these conditions. The pattern of ECP cleavage of pyrene- or DC-labeled actin (not shown) did not differ from that of unmodified actin.

S1 binding to actin

Binding of the two proteins was analyzed by measuring the rapid initial increase in the fluorescence of pyrene-labeled actin upon its mixing with S1 (Valentin-Ranc et al., 1991). To prevent S1-induced polymerization, in the fluorescence titration experiments actin was used at a low concentration (1 μM for unmodified and 1–3 μM for ECP-cleaved actin), and a separate sample of actin-S1 mixture was prepared for each experimental point. The measurements were taken 5–7 s after mixing of the proteins. Because of the instability of ECP-cleaved actin, free ATP was not removed from stock actin solutions. Aliquots of stock solutions were diluted with ATP-free buffer immediately before the measurement. Because the Ca^{2+}-activated ATPase activity of S1 is high, the 4–8 μM free ATP introduced with the actin solution was hydrolyzed within the mixing time. Plots of the relative increase in pyrene fluorescence versus S1 concentration were fitted with a single dissociation constant for S1 binding to n putatively equivalent and independent binding sites on G-actin using a computer program for nonlinear least-square analysis, DataWnd, written by A. A. Kasprzak.

Electron microscopy

All samples for electron microscopy were applied onto carbon-coated copper grids without dilution. Depending on protein concentration, protein assemblies were negatively stained with 1% (w/v) uranyl acetate either directly or after washing off excess material from the grid with a few drops of buffer G without ATP. The grids with actin polymerized by S1(A2) added together with KCl were washed with a few drops of the uranyl acetate solution instead of buffer G. Specimens were examined in a JEOL JEM 1200 EX electron microscope at an accelerating voltage of 80 kV.

For measurement of filament lengths, pictures were taken at a magnification of 6000×. Micrographs of several adjacent areas on the grid were scanned with Arcus 1200 Agfa scanner and combined into one picture using Adobe Photoshop 6.0 CE. Filament lengths were analyzed using LUCIA software (Laboratory Imaging Ltd., Prague, Czech Republic). Number average lengths, $\langle L\rangle n$, were calculated using the equation

$$\langle L\rangle n = \Sigma n_i l_i / \Sigma n_i, \quad (1)$$

where n_i is the number of filaments of length l_i. The total number of objects measured per field was 600–1300 when the filaments were short (actin polymerized by S1(A1)), and 120–200 when the filaments were long (actin polymerized by S1(A2)).

RESULTS

Effects of ECP cleavage on salt-induced polymerization of actin

In agreement with the data from the pyrene-actin fluorescence assay (Khaitlina et al., 1993), the light-scattering measurements illustrated in Fig. 2 *A* show that Ca-G-actin cleaved between residues 42 and 43 is able neither to spontaneously

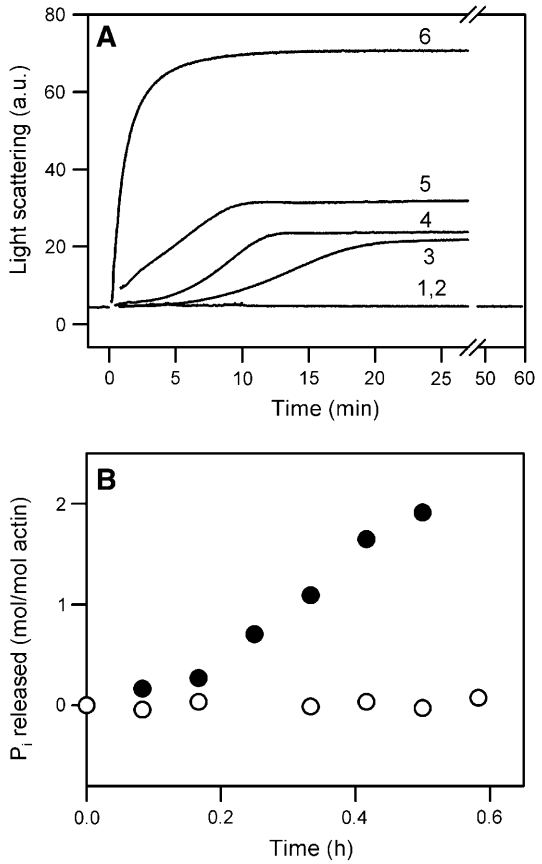

FIGURE 2 ECP-cleaved G-actin requires tightly bound Mg^{2+} for both the nucleation and filament elongation step of salt-induced polymerization. (*A*) At time zero, ECP-cleaved Ca-G-actin (24 μM) was supplemented with 0.1 M KCl (curve *1*) or with 0.1 M KCl and 0.25 μM phalloidin-stabilized F-actin seeds (see Materials and Methods) (curve *2*) and light-scattering intensity was measured at 25°C. (Curve *3*) ECP-cleaved Ca-G-actin was incubated with 0.1 M KCl for 1 h and then, at time zero, was supplemented with 0.2 mM EGTA/50 μM $MgCl_2$ to replace tightly bound Ca^{2+} with Mg^{2+}. (Curves *4* and *5*) ECP-cleaved Mg-G-actin supplemented at time zero with 0.1 M KCl alone or combined with 0.25 μM F-actin seeds, respectively. (Curve *6*) intact Mg-G-actin with 0.1 M KCl added at time zero. (*B*) ECP-cleaved Ca-G-actin (○) or Mg-G-actin (●), both 24 μM, were incubated at 25°C with 0.1 M KCl added at time zero. ATP hydrolysis was monitored by determining the released P_i using the method of Kodama et al. (1986).

polymerize in the presence of KCl (curve *1*) nor to add to the ends of phalloidin-stabilized F-actin fragments (curve *2*), and that its ability to polymerize is rescued by replacement of the tightly bound Ca^{2+} with Mg^{2+} (curves *3* and *4*). In addition, this figure also shows that the nucleation reaction of the Mg^{2+}-bound form of cleaved actin is substantially inhibited. This is apparent from a long lag phase (curves *3* and *4*), not seen with intact Mg-G-actin under the same conditions (curve *6*), and from its disappearance when polymerization is nucleated by phalloidin-stabilized seeds (curve *5*).

To better understand the nature of the polymerization defect of ECP-cleaved Ca-G-actin, in the experiment presented in Fig. 2 *B*, we examined whether incubation of this actin in the presence of 0.1 M KCl causes any change in the phosphorylation state of its bound nucleotide. In contrast to the time-dependent inorganic phosphate (P_i) release observed with the Mg^{2+}-bound form (*solid circles*), reflecting hydrolysis of the bound ATP associated with polymerization of actin, with ECP-cleaved Ca-G-actin no P_i liberation was observed (*open circles*). This observation excludes the possibility of formation of unstable, cycling oligomers. The continuation of ATP hydrolysis by Mg-actin after liberation of 1 mol P_i per mol actin is due to the enhanced steady-state subunit exchange in ECP-modified Mg-F-actin (Khaitlina and Strzelecka-Gołaszewska, 2002).

Effects of ECP cleavage on S1-induced polymerization of actin

Fig. 3 *A* compares the abilities of the S1(A1) and S1(A2) isoforms to assemble intact and ECP-cleaved Ca-G-actins into decorated filaments as monitored by measuring the increase in light-scattering intensity. The cleavage significantly reduced the rate of polymerization by S1(A1), and the increase in light-scattering intensity was preceded by a lag phase that was not seen in S1(A1)-induced polymerization of unmodified actin (compare curves *2* and *4*). The final scattering intensity (at the relatively high actin concentration and 1.5-fold molar excess of S1 over actin used in this experiment) was, however, similar to that with intact actin, and formation of decorated filaments was confirmed by electron microscopy of negatively stained preparations (Fig. 4*C*). In contrast to S1(A1), S1(A2) did not produce any change in light-scattering intensity, apart from an initial small increase reflecting S1 binding (Fig. 3 *A*, curve *1*). No further change occurred even when the concentration of the protein was increased to 50 μM each and the incubation prolonged to several hours (data not shown). The absence of S1(A2)-decorated filaments was verified by electron microscopy (Fig. 4 *D*). These results clearly show that the A1 light chain of myosin is indispensable for S1-induced polymerization of cleaved actin in the absence of salt. The joint effect of S1(A2) and 0.1 M KCl (Fig. 4 *E*) will be discussed below.

The pyrene-actin fluorescence assay for actin polymerization (Kouyama and Mihashi, 1981; Cooper et al., 1983b) revealed other distinctive features of S1-induced assembly of intact and ECP-cleaved actin into filaments (Fig. 3 *B*). Earlier studies established that the initial rapid increase in the fluorescence intensity upon addition of either S1(A1) or S1(A2) to intact Ca-G-actin (curves *3* and *4*) monitors the formation of binary GS and ternary G_2S complexes (Valentin-Ranc and Carlier, 1992; Blanchoin et al., 1995) and their association into short oligomers (Valentin-Ranc and Carlier, 1992; Fievez et al., 1997b). The lower amplitude of this initial change produced by S1(A2) reflects the slower rate of oligomer formation compared with S1(A1). It has been suggested that the subsequent sharp decrease in the intensity of pyrene fluorescence during polymerization induced by S1(A1) (not seen with S1(A2)), coinciding with filament assembly (see curve *4* in Fig. 3 *A*), reflects a structural rearrangement of the acto-S1 complexes upon actin filament formation. The final reincrease in the fluorescence, lagging behind polymerization, is linked to dissociation of P_i from the F-actin(ADP-P_i)-S1 intermediate (Fievez et al., 1997a). Similar measurements performed for ECP-cleaved actin (curves *1* and *2*) show that the initial rapid increase in fluorescence intensity upon addition of either of the two S1 isoforms is preserved, indicating that the incapability of S1(A2) to promote polymerization of cleaved actin is not due to a lack of its binding to the modified actin. The amplitude of

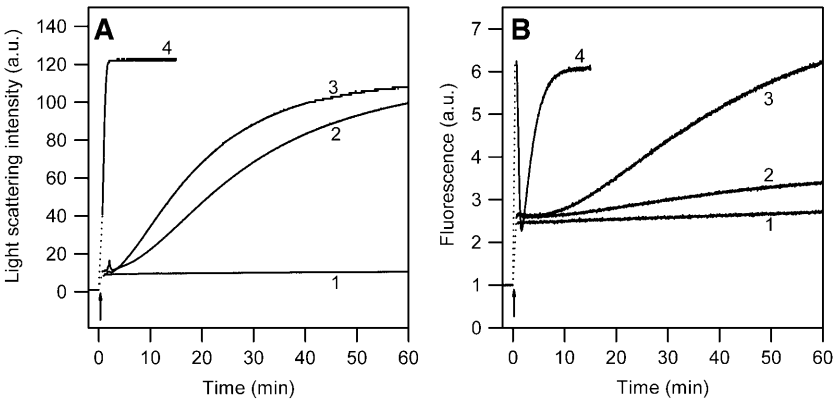

FIGURE 3 Comparison of S1-induced polymerization of ECP-cleaved and unmodified Ca-G-actin. At time zero, 15 μM (final concentration) 75% pyrene-labeled ECP-cleaved Ca-G-actin (curves *1* and *2*) or intact Ca-G-actin (curves *3* and *4*) was supplemented with 22.5 μM S1(A2) (curves *1* and *3*) or S1(A1) (curves *2* and *4*). Intensity of scattered light (*A*) and of pyrene fluorescence (*B*) were measured in parallel samples at 25°C. The possible courses of the initial increase in fluorescence intensity occurring within the time of mixing are marked with dotted lines.

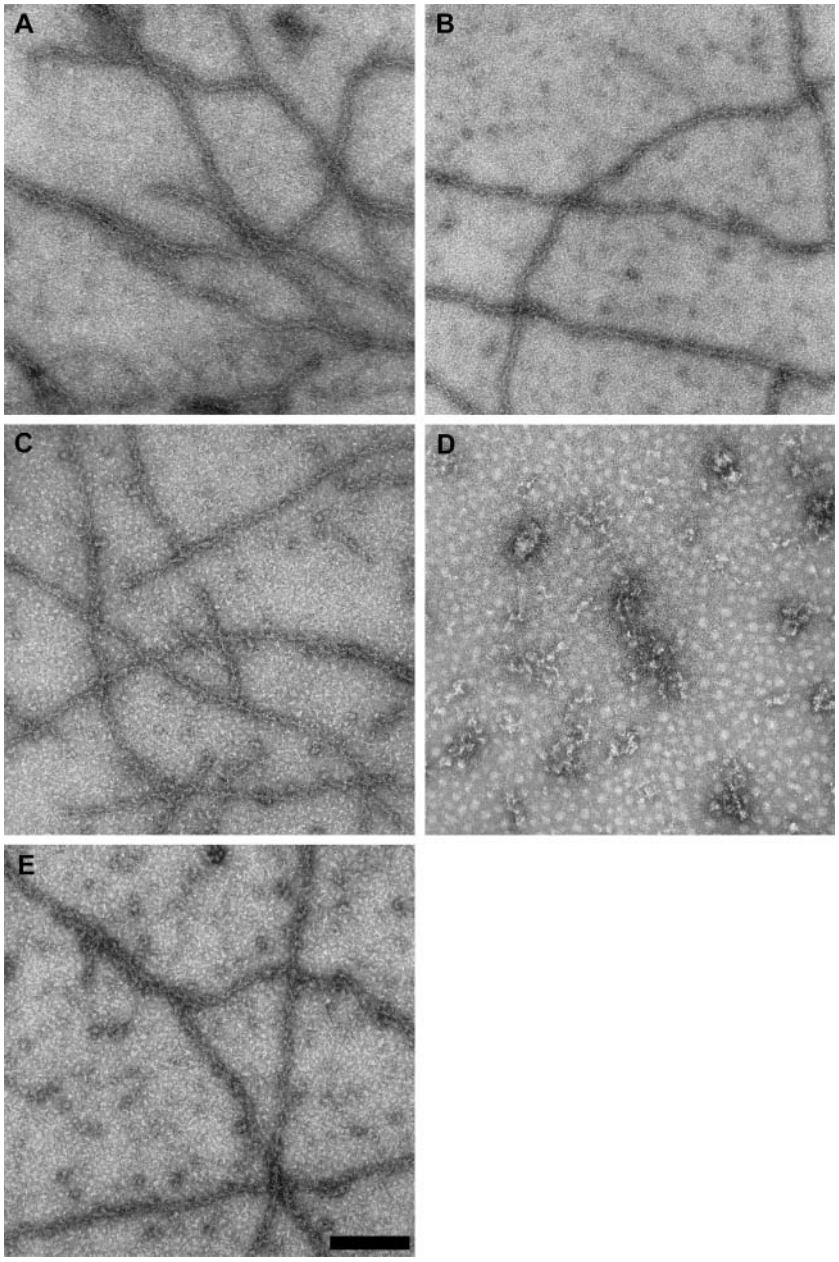

FIGURE 4 Electron micrographs of negatively stained assemblies formed by Ca-G-actin complexed with myosin subfragment 1 isoforms S1(A1) and S1(A2). Five μM intact actin (*A* and *B*) or 10 μM ECP-cleaved actin (*C–E*) were combined with S1(A1) (*A* and *C*) or S1(A2) (*B, D,* and *E*) added in a twofold molar excess, in buffer G. In *E*, 0.1 M KCl was added together with S1(A2). The progress of S1-induced polymerization of actin was monitored by measuring the intensity of scattered light at 25°C. Samples of the solutions were negatively stained after the final, constant level of light-scattering intensity was reached. The bar corresponds to 200 nm.

the S1(A1)-induced initial rapid increase in fluorescence (curve *2*) was, however, more than twofold smaller than with uncleaved actin (curve *4*) and comparable to the increase induced in both cleaved and uncleaved actin by S1(A2) (curves *1* and *3*). These differences between cleaved and intact actin might arise from a different response of the pyrene label to S1 binding, from weaker binding of S1 to cleaved actin, and/or from a diminished rate of oligomerization of cleaved G-actin-S1 complexes.

The pattern of further changes in pyrene fluorescence was also different from that observed with S1(A1)-treated uncleaved actin: the transient decrease in pyrene fluorescence was absent, and the final fluorescence increase was small and coincided with filament formation as monitored by the increase in light scattering (compare curve *2* in Fig. 3, *A* and *B*). The relatively small increase in the quantum yield of the fluorescence of the pyrene probe in ECP-cleaved actin associated with filament formation correlates with a difference in the fine structure of the fluorescence excitation spectra of cleaved and intact F-actin. As shown in Fig. 5, the second prominent peak, centered at 366 nm, that is characteristic of the excitation spectrum of unmodified F-actin, in cleaved F-actin is reduced to a shoulder on the arm of the main 345 nm peak. This additional peak was also absent from the spectrum of salt-polymerized Mg-form of ECP-cleaved actin (Khaitlina et al., 1993). As judged from steady-state light-scattering

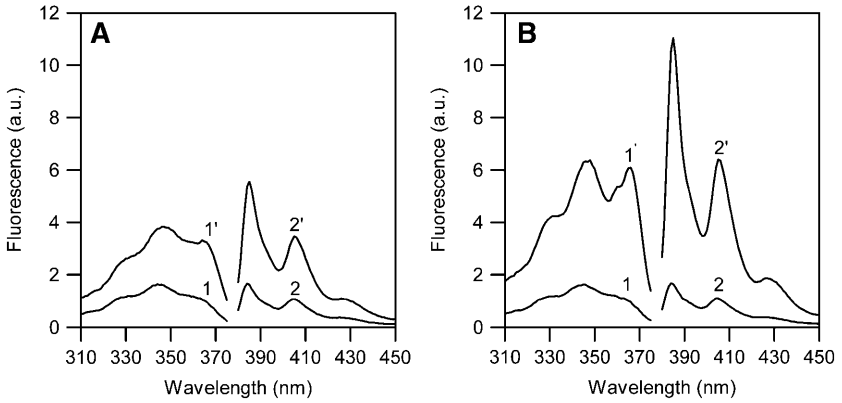

FIGURE 5 Changes in the excitation spectrum of pyrene-actin, associated with S1(A1)-induced polymerization of ECP-cleaved (*A*) and unmodified Ca-G-actin (*B*). Fluorescence excitation and emission spectra of 15 μM 75% pyrene-labeled actin were recorded at 25°C, before (curves *1* and *2*) and after (curves *1′* and *2′*) polymerization induced by addition of 30 μM S1(A1). The excitation spectra (*left*) were recorded at 407 nm, and the emission spectra (*right*) were obtained after excitation at 365 nm.

intensities, these differences are too large to be caused by different extents of polymerization, indicating cleavage-induced alterations in the filament structure.

Influence of ECP cleavage on the formation of initial G-actin-S1 complexes

The binding of both S1(A1) and S1(A2) to cleaved actin was further examined by fluorescence titration of pyrene-labeled actin with these two S1 isoforms at low actin concentrations to suppress polymerization. Fitting the plots of the relative increase in pyrene fluorescence versus S1 concentration (Fig. 6) with a single dissociation constant for S1 binding to n equivalent and independent binding sites on G-actin described by Valentin-Ranc yielded for intact actin K_d values of 50 ± 0.8 nM and 60 ± 1.9 nM (means ± SEM from four to five measurements on different protein preparations) and the average binding stoichiometry of 0.80 and 0.85 mol S1 per mol of actin for S1(A1) and S1(A2), respectively. These stoichiometries suggest formation of a mixture of GS and G_2S complexes at S1/actin ratios <1, with binary GS complexes (or their dimers, $(GS)_2$) being a predominant species under conditions of our titration experiments (initial presence of free ATP at 4–8 μM). In view of the possible difference between the fluorescence of each of the two actin molecules in ternary G_2S complexes and different equilibrium dissociation constants of GS and G_2S complexes (Valentin-Ranc et al., 1991; Kim et al., 1998), the obtained K_d values are only an approximation. Nevertheless, they are consistent with previous determinations (Valentin-Ranc et al., 1991; Lheureux et al., 1993; Kim et al., 1998).

ECP cleavage resulted in an ~4-fold increase in the K_d values for both S1(A1) and S1(A2) (to 192 ± 60 nM and 240 ± 34 nM, respectively), but no large change in the average binding stoichiometry was observed. (The best fits were obtained with 0.82 and 0.90 mol S1 per mol of actin for S1(A1) and S1(A2), respectively.) The titration data also show that the specific fluorescence of pyrene-actin in the initial G-actin-S1 complexes is similar to that of unmodified actin, and that the binding of both S1 isoforms to ECP-modified actin at the 1.5-fold molar excess of S1 used in the polymerization experiments described above was close to the saturation level of 1 mol S1 per mol of actin, indicating that the polymerization defects of cleaved actin cannot be accounted for by its diminished affinity for S1.

According to the proposed structure of the ternary G_2S, the D-loop of the second actin monomer makes contact with the monomer above it, whereas in the GS complex this loop is not involved in intermolecular interactions. Therefore, it is plausible that binding of a second actin monomer to the binary GS complex to yield G_2S (as well as association of GS into $(GS)_2$ complexes) is perturbed by ECP cleavage more strongly than the initial formation of GS complexes. S1 titration of pyrene-actin did not show it unambiguously

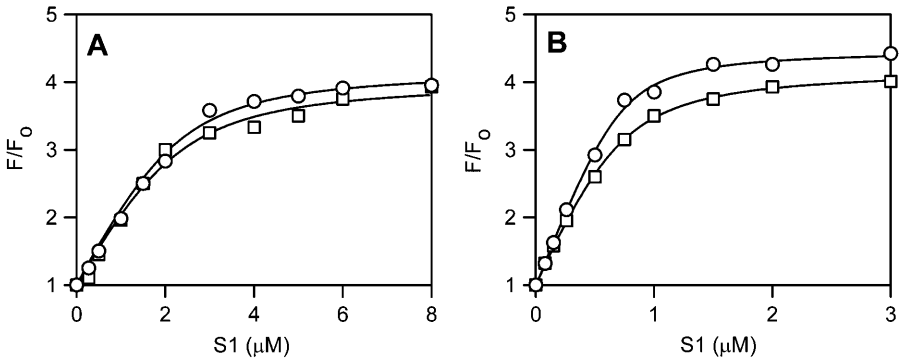

FIGURE 6 Formation of initial complexes between myosin subfragment-1 and ECP-cleaved (*A*) and unmodified (*B*) Ca-G-actin. Pyrene-labeled (20%) ECP-cleaved and unmodified Ca-G-actin at final concentrations of 3 μM and 1 μM, respectively, were titrated with S1(A1) (○) or S1(A2) (□), as described in the Materials and Methods section, at 25°C. The initial concentration of free ATP (introduced with actin) was 8.4 μM. F_0 and F denote the fluorescence of pyrene-G-actin and of the pyrene-G-actin-S1 complexes, respectively.

because, under the conditions of our experiments (the presence of micromolar concentrations of ATP, as described in Materials and Methods), G_2S complexes could not form in amounts sufficient to reveal a statistically significant effect of D-loop cleavage on their formation. Therefore, to probe the effect of this modification of actin on the transient formation of longitudinal actin dimers in the process of S1-induced polymerization, we used actin fluorescently labeled with DC at Gln^{41}. The fluorescence of this probe increases more than twice upon salt-induced actin polymerization (Takashi, 1988; Moraczewska et al., 1999). Here we examined the effects of S1 binding to DC-labeled ECP-cleaved and uncleaved G-actin at a low actin concentration (1 μM) at which polymerization is slow (see *inset* to Fig. 7) and, as will be shown below (Fig. 8, *A* and *B*), no massive formation of short oligomers is observed before polymerization. S1 was added in a twofold molar excess to first transform all actin into GS complexes.

As shown in Fig. 7, addition of S1(A1) to uncleaved actin resulted in an immediate increase in the fluorescence by ~60%, whereas with S1(A2) only a 12% increase was observed. In view of the myosin A1 light chain binding to the second actin molecule in a longitudinal actin dimer (Timson et al., 1998), the fivefold larger effect of S1(A1) compared with S1(A2) suggests that the fluorescence increase reflects a change in the environment of the label upon actin-actin contact formation in dimeric $(GS)_2$ complexes stabilized by A1 light chain. Cleavage of the D-loop did not produce

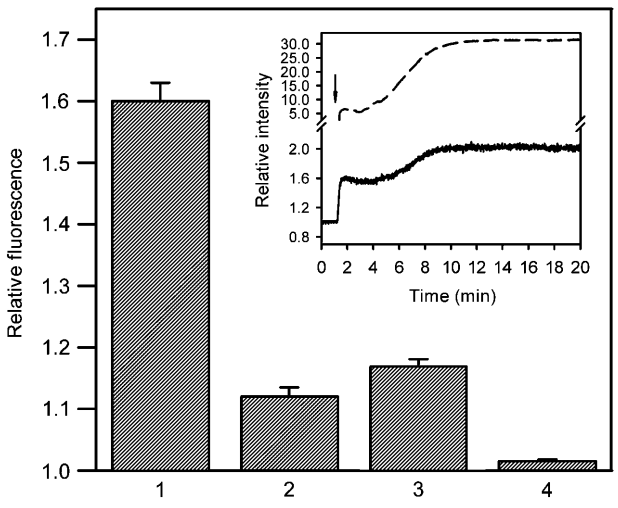

FIGURE 7 Influence of ECP cleavage on the S1(A1)- and S1(A2)-induced changes in the fluorescence of DC-labeled actin. Fluorescence intensity was recorded before and immediately after mixing of 1 μM intact Ca-G actin (*1* and *2*) or ECP-cleaved actin (*3* and *4*) (80% DC-labeled, in buffer G containing 19 μM ATP) with a twofold molar excess of S1(A1) (*1* and *3*) or S1(A2) (*2* and *4*). The inset shows the time courses of changes in DC fluorescence (*solid line*) and in light-scattering intensity at 450 nm (*dashed line*) associated with polymerization of 1 μM DC-labeled intact Ca-G actin by 2 μM S1(A1), at 25°C. The initial intensities of the fluorescence and light scattering of actin were normalized to 1.

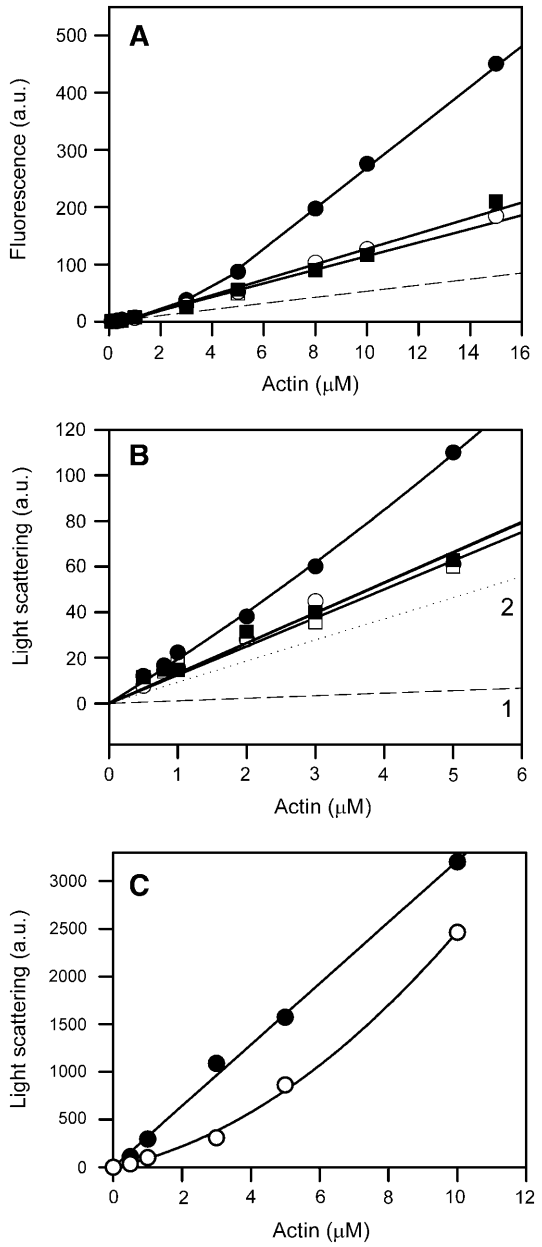

FIGURE 8 Dependence of S1-induced oligomer formation and polymerization of intact and ECP-cleaved Ca-G-actin on actin concentration. (*A* and *B*) Unmodified Ca-G-actin (*solid symbols*) and ECP-cleaved Ca-G-actin (*open symbols*) at the final concentrations indicated on the abscissa were mixed with S1(A1) (●, ○) or S1(A2) (■, □) added in a twofold molar excess, and the intensity of pyrene fluorescence (*A*, 71% pyrene-labeled actin) or scattered light (*B*, unlabeled actin) was measured at 25°C immediately (~5 s) after mixing of the proteins. The fluorescence or light-scattering intensity of actin alone is indicated by the dashed lines. The dotted line in *B* is for the intensity of light scattered by S1 alone. The initial concentration of free ATP in the mixtures was 65 μM. (*C*) Unmodified Ca-G-actin (●) and ECP-cleaved Ca-G-actin (○) at the final concentrations indicated on the abscissa were mixed with S1(A1) in a twofold molar excess over actin and allowed to polymerize at 25°C, and the final values of light-scattering intensity were measured. All samples initially contained free ATP in an 8.5-fold molar excess over actin.

a significant change in the fluorescence of DC-labeled G-actin alone (a 2–4% decrease was observed). However, it diminished the enhancement of fluorescence by S1(A1) and S1(A2) binding to only 15% and 3%, respectively. This effect of the cleavage suggests an inhibition of the association of GS complexes into $(GS)_2$ dimers or a substantial weakening of the longitudinal actin-actin contacts involving the D-loop in these dimeric complexes.

In view of the intramolecular coupling between the D-loop and the C-terminal region in subdomain 1 of actin (Crosbie et al., 1994; Kuznetsova et al., 1996), where both the S1 heavy chain and A1 light chain bind (Sutoh, 1982), the S1-induced changes in DC fluorescence might also arise, at least in part, from an intramolecular allosteric effect of S1 binding to actin. The reduction of the initial fluorescence enhancement in ECP-cleaved actin would then indicate a perturbation of the connectivity between the D-loop and subdomain 1. Nevertheless, independent of its nature, this part of the fluorescence change, which is associated with A1 light chain binding (to the second monomer in an actin dimer), must reflect formation of dimeric $(GS)_2$ complexes.

Influence of ECP cleavage on the condensation of G-actin-S1 complexes into oligomers

The effect of ECP cleavage on the next step of S1-induced polymerization of actin was investigated by measuring the magnitude of the initial rapid increase in the fluorescence of pyrene-G-actin upon addition of two equivalents of S1(A1) as a function of actin concentration (Fig. 8 *A*). In agreement with earlier studies by Carlier and her collaborators, with intact actin and S1(A1) a cooperative increase in the fluorescence intensity was seen when G-actin concentration was increased to >2 μM, indicating rapid association of the initial G-actin-S1 complexes into short oligomers (Valentin-Ranc et al., 1991). With S1(A2), the fluorescence intensity was a linear function of actin concentration up to at least 10 μM. In contrast, the changes in the fluorescence of ECP-cleaved actin combined with S1, independent of the type of the myosin light chain, did not deviate from linearity in the whole range of actin concentrations used, suggesting that cleavage of actin between residues 42 and 43 strongly inhibits the step of oligomer formation in S1-induced filament assembly. This conclusion is supported by measurements of light-scattering intensity immediately after mixing G-actin with S1. The results presented in Fig. 8 *B* show that, independent of the type of myosin essential light chain, the size and shape of objects formed from ECP-cleaved G-actin do not change with increasing actin concentration between 0.5 μM and 5 μM (the highest concentration used in this experiment), and they are different from the size and/or shape of complexes assembled from intact actin by S1(A1) that scatter light more intensely.

The light-scattering intensities after a 20-h incubation of ECP-cleaved G-actin with S1(A1) (Fig. 8 *C*) indicate formation of decorated filaments in a wide range of actin concentrations, including those at which no detectable oligomer formation was revealed by the measurements taken immediately after mixing of the two proteins. The biphasic character of the dependence of the light-scattering intensity on actin concentration is, however, consistent with the existence of a threshold concentration of G-actin-S1 complexes below which decorated filaments cannot be assembled. Fig. 8 *C* shows that this threshold concentration is higher for ECP-cleaved than for intact actin. Earlier studies on unmodified actin showed that it is also higher for the polymerization induced by the S1 isoform carrying A2 light chain than for S1(A1) (Valentin-Ranc et al., 1991; Lheureux et al., 1993).

Effects of salt on S1-induced polymerization of ECP-cleaved actin

Stabilization of the $(GS)_2$ or G_2S intermediates by the binding of the myosin A1 light chain to the second monomer in a longitudinal actin dimer (Timson et al., 1998) has been considered one of the possible mechanisms underlying faster polymerization of actin by S1(A1) than by S1(A2). The contribution of other factors to the accelerating effect of the A1 light chain was suggested based on an observation that stabilization of longitudinal actin dimers by their chemical cross-linking did not abolish the kinetic advantage of S1(A1) in inducing polymerization of these cross-linked dimers (Kim et al., 1998).

In an earlier study, it was demonstrated that S1(A2)-induced polymerization of actin is largely accelerated by KCl; this effect was attributed to compensation of the poor nucleating ability of S1(A2) by salt-induced nucleation of actin (Chen and Reisler, 1991). Such an explanation would not apply to ECP-cleaved Ca-G-actin because neither KCl alone nor S1(A2) alone is able to promote nucleation (oligomerization) of this actin. Despite this, the addition of 0.1 M KCl together with S1(A2) partially restores the ability of this actin to assemble into S1(A2)-decorated filaments as indicated by light-scattering measurements (Fig. 9 *A*) and confirmed by electron microscopic investigation of negatively stained preparations (Fig. 4 *E*). This experiment shows that the ability of cleaved actin to associate into nuclei requires either S1(A1) or a joint effect of the S1 heavy chain binding to actin and another factor that is common to KCl treatment and myosin A1 light chain binding. There seem to be two such factors, electrostatic and conformational.

Both the heavy and the A1 light chain of myosin bind to actin by electrostatic interactions with negatively charged areas on the monomer surface (Sutoh, 1982; Lheureux and Chaussepied, 1995). The A1 light chain binds through its positively charged N-terminal extension to a cluster of acidic residues in subdomain 1 of the second monomer in a longitudinal actin dimer. Neutralization of these negatively charged residues by either myosin A1 light chain binding or by Coulombic screening by dissolved ions (salt effect) may stimulate nucleation by diminishing the residual electrostatic

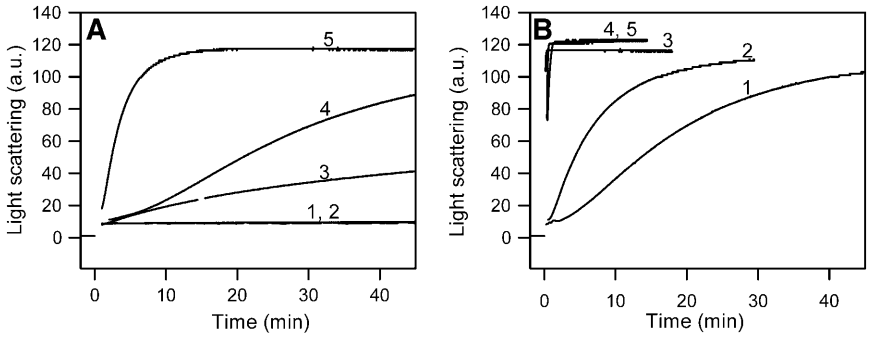

FIGURE 9 Effects of 0.1 M KCl and of substitution of Mg^{2+} for the tightly bound Ca^{2+} on the ability of ECP-cleaved (*A*) and unmodified (*B*) actin to polymerize in the presence of S1(A2). At time zero, 15 μM (final concentration) Ca-G-actin was supplemented with 30 μM S1(A2) alone (*curve 1*), S1(A2) and 0.1 M KCl added one after another (curve *3*), or S1(A1) (curve *4*), and changes in the intensity of scattered light were recorded at 25°C. In parallel samples, Ca-G-actin was converted into Mg-G-actin and the light-scattering intensity was measured after addition of 30 μM S1(A2) (curve *2*) or S1(A1) (curve *5*).

repulsion between $(GS)_2$ and between $(GS)_2$ and GS complexes. It may also contribute to stabilization of the longitudinal intermonomer contacts between subdomains 1 and 2 in the growing filaments. An alternative or additional possibility is that it triggers a change in subdomain 1 conformation that is intramolecularly transmitted to subdomain 2 and stabilizes the subdomain 2/subdomain 1 interface in the dimer, which in turn stimulates lateral contact formation with the third monomer. Whatever the mechanism, the similarity of the ionic-strength and A1 light chain effects points to the importance of the electrostatic factor.

The importance of the electrostatic effect is also substantiated by the observation that the conformational change generated when actin-bound Ca^{2+} is replaced by Mg^{2+}, which rescues salt-induced polymerization of ECP-cleaved actin, is insufficient to stimulate its polymerization by S1(A2) (Fig. 9 *A*, curve *2*), whereas polymerization by S1(A1) is markedly accelerated (compare curves *4* and *5* in Fig. 9 *A*). The fast polymerization by S1(A2) of unmodified Mg-G-actin (Fig. 9 *B*, curve *2*) excludes the possibility that the failure of this S1 isoform to polymerize ECP-cleaved Mg-G-actin reflects a long-lasting dissociation of G-actin-S1 complexes by MgATP initially present in solution because of the low MgATPase activity of myosin.

Electron microscopic investigation of the filament growth step of S1-induced polymerization of unmodified and ECP-cleaved actin

Isodesmic end-to-end association of massively formed oligomers into short filaments, followed by annealing of the latter into long filaments, was proposed by Carlier and coworkers to be a specific feature of S1-induced polymerization (Valentin-Ranc and Carlier, 1992; Fievez et al., 1997a). To test this hypothesis, we used electron microscopy to evaluate the effects of factors changing the rate of the oligomerization reaction on filament length distribution at various stages of S1-induced polymerization.

Addition of S1(A1) to 5 μM G-actin resulted in rapid formation of numerous short filaments; nearly 90% of the filaments assembled within the first 2 min were 0.05–0.1 μm long (Figs. 10 *A* and 11 *A*). With the progress in the polymerization reaction, the number average length of the filaments, $\langle L \rangle n$, increased to 0.34 μm when the polymerization was ~80% complete, and to ~1 μm at steady state, ~14 min after initiation of the reaction (Fig. 11, *B* and *C*). These observations are consistent with rapid oligomer formation but do not provide information on whether the polymers are assembled by isodesmic end-to-end association of massively formed oligomers or by their elongation by addition of successive G-actin-S1 complexes.

When 5 μM G-actin was polymerized by S1(A2), a broad and exponential distribution of the filament lengths was seen, with lengths up to ~8 μm already at the initial stage of filament assembly (~40 min after S1 addition) (Figs. 10 *D* and 11 *D*). Such long filaments are unlikely to form by a slow annealing process, which requires a diffusional encounter of two filaments, with the diffusion rate diminishing as the filament length increases. As one can see in Fig. 10, *G* and *H*, within similar time periods relatively long filaments were also assembled by S1(A1) when formation of the smallest oligomers that could serve as nuclei was slowed down by diminishing actin concentration to 1 μM or by ECP cleavage of the D-loop, respectively.

These observations support the early view that, in general, S1-induced polymerization follows the nucleation-filament growth mechanism in which G-actin-S1 complexes are preferentially added to the filament ends. The rapid formation of short decorated filaments that subsequently undergo slow end-to-end annealing is only a consequence of massive formation of the small oligomers in the presence of S1(A1) and at high actin concentrations.

A specific feature of S1-induced polymerization is a Poisson-type filament length distribution and the absence of short filaments at steady state (Fig. 11, *C* and *F*). This seems to be an effect of stabilization of both filament ends by S1 binding so that annealing is the only way filament length changes after all G-actin-S1 complexes are incorporated in the polymer.

DISCUSSION

The D-loop is the most mobile area of an actin molecule. Its rearrangement in F-actin subunits upon P_i release after the

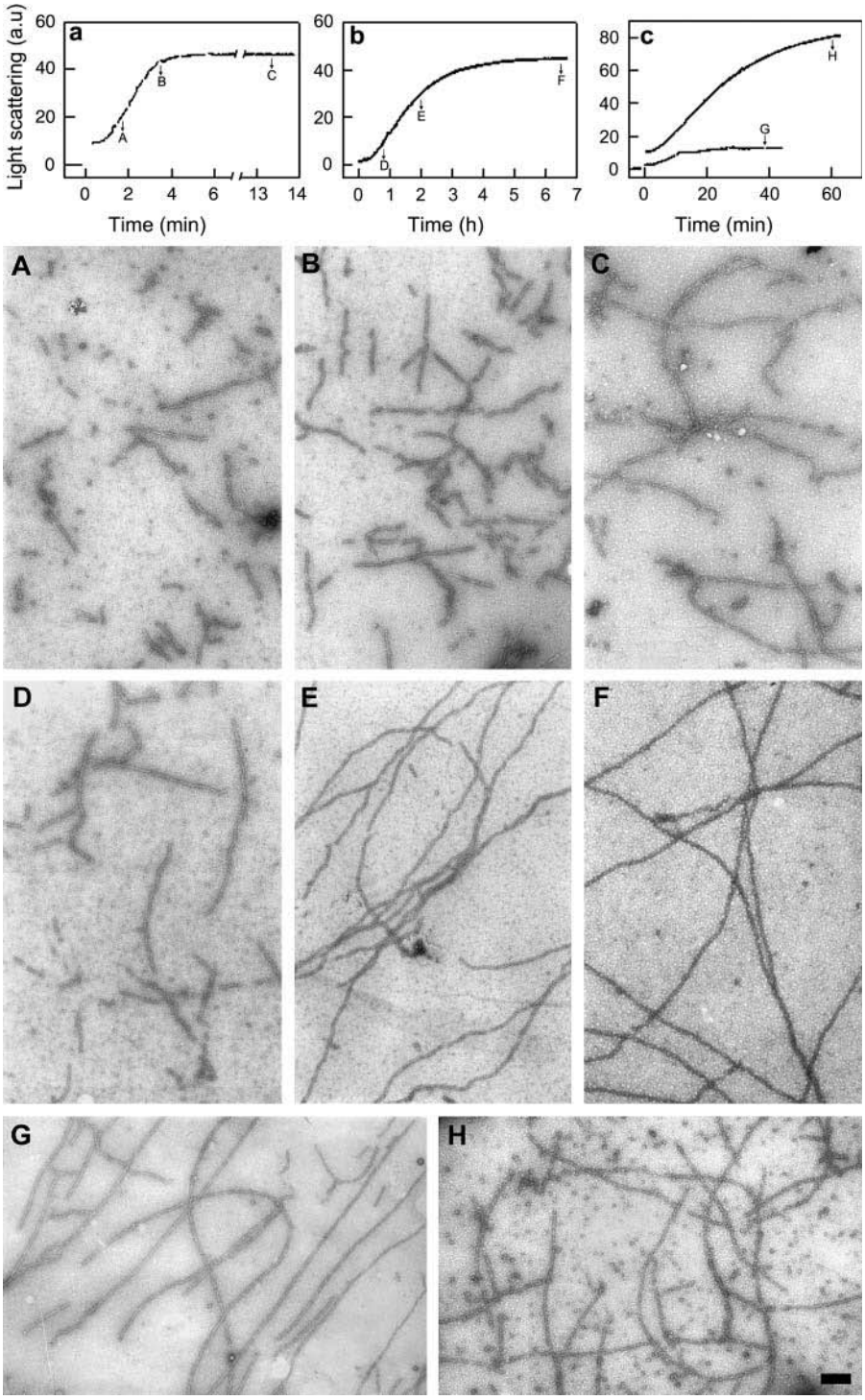

FIGURE 10 Electron micrographs of decorated filaments formed during S1-induced polymerization of Ca-G-actin. Polymerization of 5 μM Ca-G-actin (intact) was initiated by addition of 10 μM S1(A1) (graph *a* and panels *A–C*) or S1(A2) (graph *b* and panels *D–F*). The polymerization was followed as a function of time by measuring the light-scattering intensity at 25°C. At times indicated with arrows, aliquots of the solutions were withdrawn and negatively stained with uranyl acetate as described in Materials and Methods. Graph *c* and panels *G* and *H* show time courses of polymerization and electron micrographs, respectively, of 1 μM intact Ca-G-actin (curve *G* and panel *G*) and 10 μM ECP-cleaved Ca-G-actin (curve *H* and panel *H*) polymerized by two equivalents of S1(A1). The bar corresponds to 200 nm.

hydrolysis of actin-bound ATP associated with monomer addition to the filament ends correlates with a destabilization of the filament (Orlova and Egelman, 1992; Muhlrad et al., 1994). Apparently, similar nucleotide type-dependent allosteric effects on the conformation of this loop in G-actin, revealed by biochemical methods (Strzelecka-Gołaszewska et al., 1993; Muhlrad et al., 1994; Moraczewska et al., 1999) and by the recently resolved crystal structures of monomeric actin (Graceffa and Dominguez, 2003), seem to contribute to the poor polymerizability of ADP-G-actin relative to ATP-G-actin. The importance of D-loop conformation for polymerization of actin is also evident from the perturbation of the filament assembly by proteolytic cleavage of this loop by subtilisin between Met^{47} and Gly^{48}

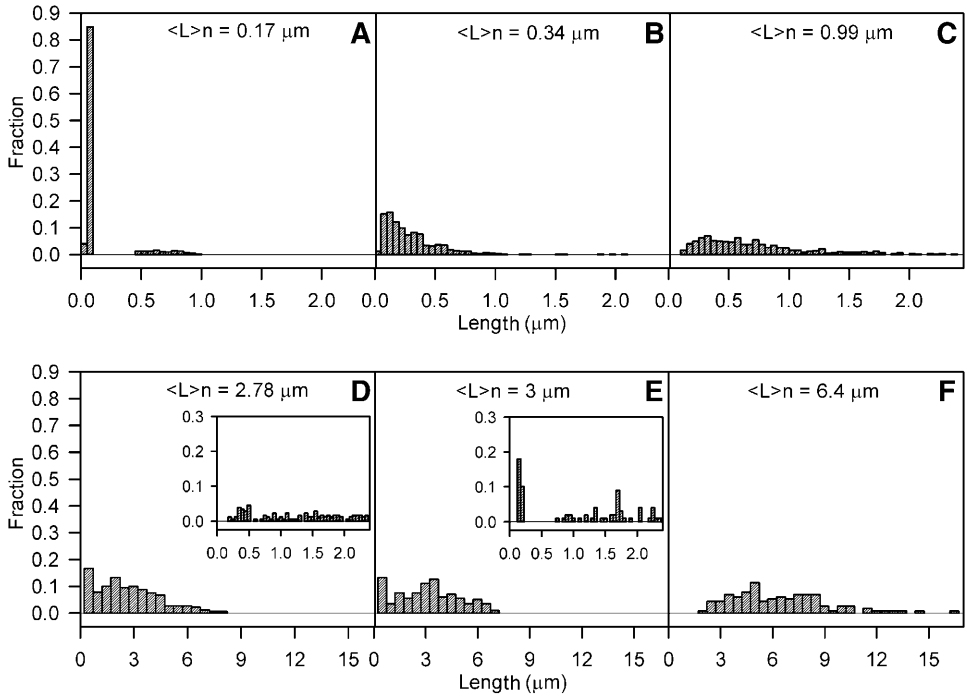

FIGURE 11 Filament length distribution at various stages of polymerization of 5 μM intact Ca-G-actin by 10 μM S1(A1) (*A–C*) or S1(A2) (*D–F*). *A–C* correspond to time points *A*, *B*, and *C* indicated in Fig. 10 *a*, and panels *D–F* refer to time points *D*, *E*, and *F* in Fig. 10 *b*. The filament lengths were measured as described in Materials and Methods.

(Schwyter et al., 1989), or by ECP cleavage between Gly^{42} and Val^{43} (Khaitlina et al., 1991 and 1993). The latter modification abolishes the ability of Ca-G-actin not only to spontaneously form nuclei in the presence of salt but also, as we show here, to elongate preformed phalloidin-stabilized nuclei.

These polymerization defects are partially reversed by replacement of the tightly bound Ca^{2+} with Mg^{2+} (Khaitlina et al., 1993, and Fig.2), which normally only accelerates the nucleation reaction and, to a much smaller extent, filament elongation (Carlier et al., 1986). An analogous effect of myosin essential A1 light chain, which strongly accelerates, but is not indispensable for, association of S1 complexes of unmodified G-actin into helical oligomers (Valentin-Ranc and Carlier, 1992), was demonstrated in this work: in the absence of salt, ECP-modified Ca-G-actin was assembled into S1-decorated filaments by the S1(A1) isoform of myosin subfragment 1 but not by S1(A2). These data indicate that D-loop conformation is of primary importance for lateral interstrand contact formation, which is rate-limiting for the nucleation reaction. This conclusion is corroborated by our examination of the effect of ECP cleavage of actin on the oligomer formation step in S1(A1)-induced polymerization. The measurements of the initial, rapid increase of light-scattering and of pyrene-actin fluorescence as a function of actin concentration at saturating S1 concentrations clearly show an inhibition of the association of G-actin-S1 complexes into oligomers (Fig. 8, *A* and *B*). A diminished rate of nuclei formation in salt-induced polymerization of cleaved actin (in the Mg^{2+}-bound form) is apparent from the prolonged lag phase preceding the increase in light-scattering intensity and from its elimination by addition of phalloidin-stabilized nuclei (Fig. 2).

It is generally accepted that the first step in nuclei/oligomer formation in both salt- and S1-induced polymerization of actin is the formation of longitudinal actin dimers. As we show here, the fluorescence of a dansyl probe attached to Gln^{41} in the D-loop is a sensitive tool for investigation of the association of G-actin-S1 complexes into dimers under conditions slowing down the subsequent oligomerization step (Fig. 7). The large increase in the fluorescence of DC-labeled actin immediately after the addition of S1(A1) indicated fast and extensive dimerization of GS complexes of unmodified actin. This is consistent with stabilization of longitudinal actin dimers by S1 heavy chain binding to both monomers (Rayment et al., 1993) and, additionally, by A1 light chain binding to the second monomer in the dimer (Timson et al., 1998). The fivefold smaller change observed with S1(A2) is consistent with a large contribution of the A1 light chain to stabilization of the dimer. The fourfold reduction of the magnitude of both the S1(A1)-induced and S1(A2)-induced change by ECP cleavage of actin suggests inhibition of the dimerization reaction upon D-loop modification. These myosin light chain-dependent changes, as well as the cleavage-induced changes, correlate with the differences in oligomer formation, indicating that destabilization of longitudinal dimers may be the primary cause of the defective polymerization of ECP-cleaved actin. These experiments, taking advantage of the extensive dimerization of S1(A1) complexes with unmodified actin, provide the first experimental evidence supporting the view that formation of the longitudinal dimer is the most critical step in the nucleation

process (Sept and McCammon, 2001). Inhibition of the nucleation reaction by weakening longitudinal actin-actin interactions between the N-terminal part of the D-loop, comprising the ECP cleavage site, and subdomain 1 of actin is in good agreement with the ''hydrophobic pocket-plug'' hypothesis of stabilization of the lateral, interstrand contacts in F-actin (Holmes et al., 1990; Lorenz et al., 1993).

Polymerization of actin requires diminishing of the electrostatic repulsive forces between the negatively charged monomers either by the charge-screening effect of salt or by binding positively charged ligands to the negative regions. The ability of S1 to assemble G-actin into decorated filaments in low-ionic strength solutions indicates that the most important step is neutralization of the negatively charged residues in subdomain 1 of actin, where both myosin heavy chain and A1 light chain are bound. The S1 heavy chain binds by means of electrostatic interactions of its positively charged residues with actin acidic residues 1–4, 24–25, and 99–100 (Combeau et al., 1992; Lheureux and Chaussepied, 1995). The A1 light chain binds through lysine residues in its N-terminal extension to the acidic residues Glu^{361}, Asp^{363}, and Glu^{364} near the C-terminus of actin (Sutoh, 1982). Our results suggest that neutralization of the cluster of acidic residues near the C-terminus and/or a change in actin conformation triggered by it contribute to the acceleration of polymerization by myosin A1 light chain and that these factors become critical when the intermonomer interaction between the D-loop and the C-terminus is weakened by ECP cleavage of the loop. This is indicated by the incapability of S1(A2) alone or KCl alone to polymerize ECP-cleaved Ca-G-actin, whereas addition of either S1(A1), or S1(A2) together with 0.1 M KCl, leads to filament assembly (Fig. 9 *A*). Since A1 light chain binds to the second monomer in a longitudinal actin dimer, it can only influence the rate of steps subsequent to dimerization of GS complexes. Neutralization of electrostatic forces opposing lateral association of a $(GS)_2$ dimer with GS, or a conformational effect facilitating it, are both likely to contribute to the acceleration of the oligomerization reaction.

S1 titrations of pyrene-actin reveal a rapid change in actin conformation, at or in the vicinity of the C-terminus, linked to S1 heavy chain binding and little sensitivity of this probe to A1 light chain binding. The role of a conformational change generated by S1 heavy chain is evident from the fact that polymerization of ECP-cleaved Ca-G-actin, which is able neither to spontaneously nucleate nor to elongate preformed nuclei in the presence of 0.1 M KCl alone, can be rescued either by exchanging actin-bound Ca^{2+} for Mg^{2+} or by addition of S1(A2) together with salt (Fig. 9 *A*). These data suggest that, similar to salt-induced polymerization, the filament assembly by S1 involves an initial ''monomer activation'' step transforming G-actin into polymerizable species (Carlier, 1991). Experimental evidence for both S1 heavy chain- and A1 light chain-dependent transitions in G-actin and their comparison with the tightly bound divalent cation-dependent and ionic strength-dependent changes in G-actin conformation will be presented elsewhere (B. Wawro, S. Yu. Khaitlina, and H. Strzelecka-Gołaszewska, unpublished).

Our measurements of the changes in filament length distribution in the course of S1-induced polymerization (Figs. 10 and 11) suggest that not only the rate but also the mode of filament assembly depends on the rate of association of G-actin-S1 complexes into the smallest helical oligomers. Isodesmic end-to-end association of the oligomers into short filaments that subsequently form longer filaments by end-to-end annealing (Valentin-Ranc and Carlier, 1992; Fievez et al., 1997a) may prevail under conditions leading to massive oligomer formation as observed with S1(A1) at high protein concentrations. This mode of filament assembly can be accommodated within the general mechanism of nucleation-filament growth as a natural consequence of the very strong acceleration of the oligomerization step by myosin A1 light chain binding to actin. The much broader, exponential distribution of filament lengths and the relatively fast appearance of long filaments indicate that elongation of oligomers by addition of G-actin-S1 complexes is the predominant pathway in polymerization initiated by S1(A2) as well as in polymerization induced by S1(A1) when the oligomer step is slowed down by lowering actin concentration or by D-loop cleavage. The nucleation-elongation mechanism is also supported by evidence from a study on cross-linked actin dimers showing preferable addition of GS rather than G_2S, $(GS)_2$, or their oligomers to the filament ends (Kim et al., 1998).

In conclusion, our results suggest that proteins triggering actin polymerization make use of the activation-nucleation-elongation mechanism in which both the overall rate of polymerization and filament length distribution are determined by the kinetics of the nucleation step. We provide experimental evidence showing the critical role of the conformation of the D-loop in subdomain 2 of actin in both longitudinal and lateral actin-actin contact formation in the nucleation reaction. These results point to allosteric effects of actin-binding proteins on the conformation of actin D-loop as a likely way of modulation of the rate of de novo filament formation in the cell.

We are grateful to Dr. Alevtina Morozova (Institute of Cytology, St Petersburg, Russia) for her gift of protease ECP32, and to Dr. Maria Filek (The F. Górski Institute of Plant Physiology of the Polish Academy of Sciences, Kraków, Poland) for access to LUCIA software. The excellent technical assistance of Mrs. Emilia Karczewska is also gratefully acknowledged.

This work was supported by grant 6 P04A 01417 (to H.S.-G.) and a statutory grant to the Nencki Institute from the State Committee for Scientific Research (Poland), and by the RAS Program on Cell and Molecular Biology and RFBR grant 02-04-48253 (to S.Yu.K).

REFERENCES

Blanchoin, L., S. Fievez, F. Travers, M.-F. Carlier, and D. Pantaloni. 1995. Kinetics of the interaction of myosin subfragment-1 with G-actin. Effect of nucleotides and DNaseI. *J. Biol. Chem.* 270:7125–7133.

Carlier, M.-F. 1991. Actin: protein structure and filament dynamics. *J. Biol. Chem.* 266:1–4.

Carlier, M.-F., and D. Pantaloni. 1997. Control of actin dynamics in cell motility. *J. Mol. Biol.* 269:459–467.

Carlier, M.-F., D. Pantaloni, and E. D. Korn. 1986. Fluorescence measurements of the binding of cations to high-affinity and low-affinity sites on ATP-G-actin. *J. Biol. Chem.* 261:10778–10784.

Chen, T., M. Heigentz, and E. Reisler. 1992. Myosin subfragment-1 and structural elements of G-actin: effects of S-1(A2) on sequences 39–52 and sequences 61–69 in subdomain-2 of G-actin. *Biochemistry.* 31:2941–2946.

Chen, T., and E. Reisler. 1991. Interactions of myosin subfragment-1 isozymes with G-actin. *Biochemistry.* 30:4546–4552.

Combeau, C., D. Didry, and M.-F. Carlier. 1992. Interaction between G-actin and myosin subfragment-1 probed by covalent cross-linking. *J. Biol. Chem.* 267:14038–14046.

Cooper, J. A., E. L. Buhle, S. B. Walker, T. Y. Tsong, and T. D. Pollard. 1983a. Kinetic evidence for a monomer activation step in actin polymerization. *Biochemistry.* 22:2193–2202.

Cooper, J. A., S. B. Walker, and T. D. Pollard. 1983b. Pyrene actin: documentation of the validity of a sensitive assay for actin polymerization. *J. Muscle Res. Cell Motil.* 4:253–262.

Crosbie, R. H., C. Miller, P. Cheung, T. Goodnight, A. Muhlrad, and E. Reisler. 1994. Structural connectivity in actin: effect of C-terminal modifications on the properties of actin. *Biophys. J.* 67:1957–1964.

Egelman, E. H., and A. Orlova. 1995. New insights into actin filament dynamics. *Curr. Opin. Struct. Biol.* 5:172–180.

Feng, L., E. Kim, W.-L. Lee, C. J. Miller, B. Kuang, E. Reisler, and P. A. Rubenstein. 1997. Fluorescence probing of yeast actin subdomain 3/4 hydrophobic loop 262–274. *J. Biol. Chem.* 272:16829–16837.

Fievez, S., M.-F. Carlier, and D. Pantaloni. 1997a. Mechanism of myosin subfragment-1-induced assembly of CaG-actin and MgG-actin into F-actin-S_1-decorated filaments. *Biochemistry.* 36:11843–11850.

Fievez, S., D. Pantaloni, and M.-F. Carlier. 1997b. Kinetics of myosin subfragment-1-induced condensation of G-actin into oligomers, precursors in the assembly of F-actin–S_1. Role of the tightly bound metal ion and ATP hydrolysis. *Biochemistry.* 36:11837–11842.

Frieden, C. 1983. Polymerization of actin: mechanism of the Mg^{2+}-induced process at pH 8 and 20 °C. *Proc. Natl. Acad. Sci. USA.* 80:6513–6517.

Graceffa, P., and R. Dominguez. 2003. Crystal structure of monomeric actin in the ATP state. Structural basis of nucleotide-dependent actin dynamics. *J. Biol. Chem.* 278:34172–34180.

Holmes, K. C., D. Popp, D. Gebhard, and W. Kabsch. 1990. Atomic model of the actin filament. *Nature.* 347:44–49.

Houk, W. T., and K. Ue. 1974. The measurement of actin concentration in solution: a comparison of methods. *Anal. Biochem.* 62:66–74.

Kasai, M., S. Asakura, and F. Oosawa. 1962. The cooperative nature of G–F transformation of actin. *Biochim. Biophys. Acta.* 57:22–31.

Kasprzak, A. A. 1993. Myosin subfragment 1 inhibits dissociation of nucleotide and calcium from G-actin. *J. Biol. Chem.* 268:13261–13266.

Khaitlina, S. Yu., J. H. Collins, I. M. Kuznetsova, V. P. Pershina, I. G. Synakevich, K. K. Turoverov, and A. M. Usmanova.1991. Physicochemical properties of actin cleaved with bacterial protease from *E. coli* A2 strain. *FEBS Lett.* 279:49–51.

Khaitlina, S. Y., J. Moraczewska, and H. Strzelecka-Gołaszewska. 1993. The actin/actin interactions involving the N-terminus of the DNase-I-binding loop are crucial for stabilization of the actin filament. *Eur. J. Biochem.* 218:911–920.

Khaitlina, S. Yu., and H. Strzelecka-Gołaszewska. 2002. Role of the DNase-I-binding loop in dynamic properties of actin filament. *Biophys. J.* 82:321–334.

Kim, E., M. Phillips, G. Hegyi, A. Muhlrad, and E. Reisler. 1998. Intrastrand cross-linked actin between Gln-41 and Cys-374. II. Properties of cross-linked oligomers. *Biochemistry.* 37:17793–17800.

Kim, E., and E. Reisler. 1996. Intermolecular coupling between loop 38–52 and the C- terminus in actin filaments. *Biophys. J.* 71:1914–1919.

Kim, E., and E. Reisler. 2000. Intermolecular dynamics and function in actin filaments. *Biophys. Chem.* 86:191–201.

Kim, E., W. Wriggers, M. Phillips, K. Kokabi, P. A. Rubenstein, and E. Reisler. 2000. Cross-linking constraints on F-actin structure. *J. Mol. Biol.* 299:421–429.

Kodama, T., K. Fukui, and K. Kometani. 1986. The initial phosphate burst in ATP hydrolysis by myosin and subfragment-1 as studied by a modified Malachite Green method for determination of inorganic phosphate. *J. Biochem.(Tokyo)* 99:1465–1472.

Kouyama, T., and K. Mihashi. 1981. Fluorimetry study of N-(1-pyrene)iodoacetamide-labeled F-actin. Local structural change of actin protomer both on polymerization and on binding of heavy meromyosin. *Eur. J. Biochem.* 114:33–38.

Kuznetsova, I., O. Antropova, K. Turoverov, and S. Khaitlina. 1996. Conformational changes in subdomain 1 of actin induced by proteolytic cleavage within the DNase-I-binding loop: Energy transfer from tryptophan to AEDANS. *FEBS Lett.* 383:105–108.

Laemmli, U. K. 1970. Cleavage of structural proteins during the assembly of the head of bacteriophage T4. *Nature.* 227:680–685.

Lheureux, K., and P. Chaussepied. 1995. Comparative studies of the monomeric and filamentous actin-myosin head complexes. *Biochemistry.* 34:11435–11444.

Lheureux, K., T. Forné, and P. Chaussepied. 1993. Interaction and polymerization of the G-actin-myosin head complex: effect of DNase-I. *Biochemistry.* 32:10005–10014.

Lorenz, M., D. Popp, and K. C. Holmes. 1993. Refinement of the F-actin model against X-ray fiber diffraction data by the use of a directed mutation algorithm. *J. Mol. Biol.* 234:826–836.

Margossian, S. S., and S. Lowey. 1982. Preparation of myosin and its subfragments from rabbit skeletal muscle. *Methods Enzymol.* 85:55–71.

Miller, L., M. Phillips, and E. Reisler. 1988. Polymerization of G-actin by myosin subfragment 1. *J. Biol. Chem.* 263:1996–2002.

Moraczewska, J., B. Wawro, K. Seguro, and H. Strzelecka-Gołaszewska. 1999. Divalent cation-, nucleotide-, and polymerization-dependent changes in the conformation of subdomain 2 of actin. *Biophys. J.* 77: 373–385.

Muhlrad, A., P. Cheung, B. C. Phan, C. Miller, and E. Reisler. 1994. Dynamic properties of actin. Structural changes induced by beryllium fluoride. *J. Biol. Chem.* 269:11852–11858.

Oosawa, F., and M. Kasai. 1962. Theory of linear and helical polymerization of macromolecules. *J. Mol. Biol.* 4:10–21.

Orlova, A., and E. H. Egelman. 1992. Structural basis for the destabilization of F-actin by phosphate release following ATP hydrolysis. *J. Mol. Biol.* 227:1043–1053.

Rayment, I., H. M. Holden, M. Whittaker, C. B. Yohn, M. Lorenz, K. C. Holmes, and R. A. Milligan. 1993. Structure of the actin-myosin complex and its implications for muscle contraction. *Science.* 261:58–65.

Schwyter, D., M. Phillips, and E. Reisler. 1989. Subtilisin-cleaved actin: polymerization and interaction with myosin subfragment 1. *Biochemistry.* 28:5889–5895.

Sept, D., and J. A. McCammon. 2001. Thermodynamics and kinetics of actin filament nucleation. *Biophys. J.* 81:667–674.

Spudich, J. A., and S. Watt. 1971. The regulation of skeletal muscle contraction. I. Biochemical studies of the interaction of the tropomyosin-troponin complex with actin and the proteolytic fragments of myosin. *J. Biol. Chem.* 246:4866–4871.

Strzelecka-Gołaszewska, H., J. Moraczewska, S. Y. Khaitlina, and M. Mossakowska. 1993. Localization of the tightly bound divalent-cation-dependent and nucleotide-dependent conformation changes in G-actin using limited proteolytic digestion. *Eur. J. Biochem.* 211:731–742.

Sutoh, K. 1982. Identification of myosin-binding sites on the actin sequence. *Biochemistry.* 21:3654–3661.

Takashi, R. 1988. A novel actin label: a fluorescent probe at glutamine-41 and its consequences. *Biochemistry.* 27:938–943.

Timson, D. J., H. R. Trayer, and I. P. Trayer. 1998. The N-terminus of A1-type myosin essential light chains binds actin and modulates myosin motor function. *Eur. J. Biochem.* 255:654–662.

Tirion, M. M., D. ben-Avraham, M. Lorenz, and K. C. Holmes. 1995. Normal modes as refinement parameters for the F-actin model. *Biophys. J.* 68:5–12.

Trayer, H. R., and I. P. Trayer. 1988. Preparation of myosin and its subfragments from rabbit skeletal muscle. *Biochemistry.* 27:5718–5727.

Valentin-Ranc, C., and M.-F. Carlier. 1992. Characterization of oligomers as kinetic intermediates in myosin subfragment 1-induced polymerization of G-actin. *J. Biol. Chem.* 267:21543–21550.

Valentin-Ranc, C., C. Combeau, M.-F. Carlier, and D. Pantaloni. 1991. Myosin subfragment-1 interacts with two G-actin molecules in the absence of ATP. *J. Biol. Chem.* 266:17872–17879.